

Herschel limits on far infrared emission from circumstellar dust around nearby Type Ia supernovae

Joel Johansson,¹ Rahman Amanullah,¹ Ariel Goobar,¹

¹*Oskar Klein Centre, Stockholm University, SE 106 91 Stockholm, Sweden*

Submitted 2012 Xxxxx XX

ABSTRACT

We report upper limits on dust emission at far infrared wavelengths from three nearby Type Ia supernovae: SNe 2011by, 2011fe and 2012cg. Observations were carried out at 70 μm and 160 μm with the *Photodetector Array Camera and Spectrometer* (PACS) on board the Herschel Space Observatory. None of the supernovae were detected in the far-IR, allowing us to place upper limits on the amount of pre-existing dust in the circumstellar environment. Due to its proximity, SN 2011fe provides the tightest constraints, $M_{\text{dust}} \lesssim 7 \times 10^{-3} M_{\odot}$ at a 3σ -level for dust temperatures $T_{\text{dust}} \sim 500$ K assuming silicate or graphite dust grains of size $a = 0.1 \mu\text{m}$. For SNe 2011by and 2012cg the corresponding upper limits are less stringent, with $M_{\text{dust}} \lesssim 10^{-1} M_{\odot}$ for the same assumptions.

Key words: ISM: dust, extinction – supernovae: general - circumstellar matter – supernovae: individual: SN 2011by, SN 2011fe, SN 2012cg

1 INTRODUCTION

The use of Type Ia supernovae (SNe Ia) as distance indicators remains essential for the study of the expansion history of the Universe and for explorations of the nature of dark energy (Goobar & Leibundgut 2011). However, a lack of understanding of the progenitor systems and the requirement for empirically derived colour-brightness corrections represent severe limitations for precision cosmology. Information about the progenitor systems of SNe Ia can be obtained by searching for evidence of circumstellar material (CSM) associated with mass-loss prior to the explosion. In the single-degenerate model, a white dwarf (WD) accretes mass from its hydrogen-rich companion star until it reaches a mass close to the Chandrasekhar mass, at which point carbon ignites triggering a thermonuclear explosion. In the double-degenerate model, a supernova results from the merger of two WDs. Thus, the detection of CSM arising from the transfer of matter to the WD by its non-degenerate binary companion would be a direct confirmation of the single-degenerate scenario. Dust may also be created in the circumstellar environment before the explosion, which would have important implications for observed colours of SNe Ia. This second scenario is the focus of this paper.

2 CIRCUMSTELLAR MATERIAL AND TYPE IA SUPERNOVAE

The existence of CSM around nearby SNe Ia has been suggested by studies of sodium absorption lines (e.g. SNe

1999cl, 2006X and 2007le, Patat et al. 2007; Blondin et al. 2009; Simon et al. 2009; Sternberg et al. 2011). High-resolution spectra reveal the presence of time-variable and blueshifted Na I D features, possibly originating from CSM within the progenitor system. Studies of large samples of SNe Ia (Sternberg et al. 2011) find that half of all SNe Ia with detectable Na I D absorption at the host-galaxy redshift have Na I D line profiles with significant blueshifted absorption relative to the strongest absorption component, which indicates that a large fraction of SN Ia progenitor systems have strong outflows. Foley et al. (2012) also find that SNe Ia with blueshifted circumstellar/interstellar absorption systematically exhibit higher ejecta velocities and redder colours at maximum brightness relative to the rest of the SN Ia population.

Non-standard reddening has been noted in studies of individual and large samples of SNe Ia. E.g., the colour excess indices of SN 2006X were studied in Folatelli et al. (2010), showing that the reddening is incompatible with the average extinction law of the Milky Way. Their findings augmented the large body of evidence indicating that the reddening of many SNe Ia show a steeper wavelength dependence ($R_V < 3.1$) than that which is typically observed for stars in our Galaxy. Previously, Nobili & Goobar (2008) derived $R_V = 1.75 \pm 0.27$ from a statistical study of 80 low redshift SNe Ia. Similarly, when the colour-brightness relation is fitted jointly with cosmological parameters in the SNe Ia Hubble diagram, using a wide range of SNe Ia redshifts, low values of R_V (or β for the SALT lightcurve fitter) are

obtained (see e.g. Suzuki et al. 2012, for a recent compilation).

Wang (2005) and Goobar (2008) showed that multiple scattering on circumstellar (CS) dust could potentially help to explain the low values of $R_V \sim 1.5 - 2.5$ observed in the sight lines of nearby SNe Ia. Amanullah & Goobar (2011) simulated the impact of thin CS dust shells located at radii $r_d \sim 10^{16} - 10^{19}$ cm ($\sim 0.003 - 3$ pc) from the SN, containing masses $M_{\text{dust}} \sim 10^{-4} M_\odot$, and find that this scenario would also perturb the optical lightcurve shapes and introduce “intrinsic” colour variations $\sigma_{E(B-V)} \sim 0.05 - 0.1$. If significant amounts of UV/optical photons from the SN are absorbed, thermal re-emission at IR wavelengths could be the “smoking gun” for the presence of CS dust. Gomez et al. (2012) report the detection of $\sim 3 - 9 \times 10^{-3} M_\odot$ of warm dust (~ 90 K) in the Kepler and Tycho supernova remnants (thought to have been created by Type Ia SNe). Their findings are consistent with the warm dust originating in the circumstellar (Kepler) and interstellar (Tycho) material swept up by the primary blast wave of the remnant. Gerardy et al. (2007) observed two normal SNe Ia (SNe 2003hv and 2005df) at late phases ($\sim 100 - 400$ days after explosion) with the *Spitzer Space Telescope*. The mid-IR spectral energy distributions (SEDs) and photometry are compatible with strong atomic line emission from the SN, and therefore exhibit no compelling indication of pre-existing or newly formed dust. Nozawa et al. (2011) model the formation of dust grains in SNe Ia ejecta and find that significant amounts of dust could condense after $\sim 100 - 300$ days after the explosion. They compare their models with the mid-IR photometry in Gerardy et al. (2007) and find that at most $\sim 0.03 - 0.075 M_\odot$ of newly formed silicate dust is consistent with the observations.

The interaction of the SN Ia ejecta with the CSM would probably also produce detectable radio and UV/X-ray emission, but as yet, observational constraints at these wavelengths are restricted to upper limits. VLA radio observations in the frequency range 4.8-43 GHz of 27 nearby SNe Ia have been analysed by Panagia et al. (2006) and Hancock et al. (2011). Most of the SNe were observed within months after the explosion. No detections were made at a mJy sensitivity and the resultant upper limits are generally consistent with pre-SN mass-loss rates $\dot{M} \lesssim 10^{-7} M_\odot \text{ yr}^{-1}$. Shocks formed by the interaction of the SN with the surrounding CSM, may heat ambient material to very high temperatures ($\sim 10^6 - 10^7$ K) producing thermal X-ray emission. Immler et al. (2006) and Russell & Immler (2012) consider a large number of SNe Ia observed using the *Swift* X-Ray Telescope. The observations were carried out at epochs between $\sim 2 - 1000$ days after discovery. None of the SNe Ia were detected in individual exposures or in the stacked images. The combined 3σ upper limit on the mass-loss rate is $\dot{M} \lesssim 10^{-6} (v_{\text{wind}}/10 \text{ km/s}) M_\odot \text{ yr}^{-1}$. Although these upper limits on the mass-loss rates are model dependent, they rule out a large portion of the parameter space of single-degenerate progenitor models.

In this paper, we present the results of our search for far-IR emission from pre-existing CS dust around Type Ia supernovae. Thus, our study is complementary to observations at other wavelengths.

3 TARGETS AND OBSERVATIONS

To search for far-IR emission from pre-existing CS dust, we targeted three Type Ia SNe: SNe 2011by, 2011fe and 2012cg. These targets were selected based on their close proximity, and the observations were made at early phases ($\lesssim 1$ month after peak) to avoid confusion due to the potential formation of new dust. Only one of these three SNe showed significant reddening at optical wavelengths, thus making a detection at far-IR wavelengths more challenging.

3.1 Herschel PACS data

The observations of SNe 2011by, 2011fe and 2012cg were obtained using the *Photodetector Array Camera and Spectrometer* (PACS) on board the Herschel satellite (Poglitsch et al. 2010; Pilbratt et al. 2010). The mini scan-map observing mode was used with a scan speed of $20''/\text{s}$, resulting in a final map of $3' \times 7'$ with a homogeneous coverage in the central region (about $50''$ in diameter). The full width at half maximum (FWHM) of the point spread function (PSF) at $70 \mu\text{m}$ and $160 \mu\text{m}$ are $6''$ and $12''$ respectively. The flux calibration uncertainty for PACS is currently estimated as 10% for the $70 \mu\text{m}$ band and 20% for the $160 \mu\text{m}$ band. The data reduction was performed up to level2 using the *Herschel Interactive Processing Environment* (HIPE). Each target was observed for 4 hours, with simultaneous imaging in the $70 \mu\text{m}$ and $160 \mu\text{m}$ bands resulting in a 5σ point source flux limit of approximately 5 and 10 mJy respectively.

In addition to our observations we also include analysis of archival data of the host galaxies of SNe 2011fe (M101 observed in 2010 June 16, PI: R. Kennicutt) and 2012cg (NGC 4424 observed in 2011 July 24, PI: J. Davie). These observations were carried out in the largeScan-mode, with a medium scan map rate of $20''/\text{s}$ resulting in maps with a $3.2''/\text{pixel}$ resolution and a 5σ point source flux limit of approximately 25 mJy in the $70 \mu\text{m}$ band.

Photometry was performed by using a set of single apertures (with radii defined by the FWHM of the PSF) to estimate the flux at the SN positions, in the vicinity of the SNe and the average sky background.

3.2 SN 2011by

SN 2011by was discovered 2011/04/26.823 by Zhangwei Jin and Xing Gao at R.A. = 11:55:45.56, Decl. = +55:19:33.8 located $5''.3$ East and $19''.1$ North of the center of the barred spiral galaxy NGC 3972 at a distance of 18.5 ± 0.8 Mpc (Tully et al. 2009). SN 2011by was classified as a normal Type Ia SN with negligible reddening (Vallery Stanishev, private communication).

Our PACS observations from 2011 May 24 (about two weeks after *B*-band maximum) are shown in Fig. 3. The SN exploded in a region of significant host galaxy background emission. To derive upper limits on possible emission from pre-existing CS dust, we compare the flux at the SN position with the estimated host galaxy background flux in the absolute vicinity (Tab. 1). The galactic emission was estimated by placing apertures along iso-flux contours. We measure no significant excess far-IR emission with respect to the estimated host galaxy background at the location of SN 2011by (3.7 ± 1.5 mJy at $70 \mu\text{m}$).

3.3 SN 2011fe

SN 2011fe was discovered 2011/08/24.000 by the Palomar Transient Factory at R.A. = 14:03:05.81, Decl. = +54:16:25.4 (J2000) located $58''.6$ West and $270''.7$ South of the center of the nearby spiral galaxy M101 (the “Pinwheel galaxy”) at a distance of 6.4 ± 0.5 Mpc (Shappee & Stanek 2011). The SN reached a peak B -band magnitude of ~ 10 on around September 10 (Matheson et al. 2012). The Galactic and host galaxy reddening, deduced from the integrated EWs of the Na I D lines are $E(B-V)_{\text{MW}} = 0.011 \pm 0.002$ and $E(B-V)_{\text{host}} = 0.014 \pm 0.002$ mag, respectively (Patat et al. 2011).

By analysing pre-explosion *HST* and *Spitzer* images, Li et al. (2011) and Nugent et al. (2011) are able to put stringent limits on the luminosity of the companion star, ruling out red-giants and a majority of helium stars as the mass donating companion to the exploding WD. Early phase radio and X-ray observations (Horeh et al. 2012; Chomiuk et al. 2012; Margutti et al. 2012) report non-detections, yielding constraints on the pre-explosion mass-loss rate from the progenitor system $\dot{M} \lesssim 6 \times 10^{-10} - 10^{-8} (v_{\text{wind}}/100 \text{ km/s}) M_{\odot} \text{yr}^{-1}$. Although they are model dependent, these limits rule out a large portion of the parameter space of single-degenerate progenitor models for SN 2011fe.

Patat et al. (2011) studied the properties of the SN environment using multi-epoch, high-resolution spectroscopy. The absence of time-variant, blueshifted absorption features rules out the presence of substantial amounts of CSM. In summary, previous observations are consistent with the progenitor of SN 2011fe being a binary system with a main sequence or a degenerate companion star.

Our Herschel PACS $70 \mu\text{m}$ and $160 \mu\text{m}$ data from 2011 October 02 (about 33 days after B -band maximum) are shown in Fig. 3. SN 2011fe is located in a region with low host galaxy background emission. No excess far-IR emission is detected at the position of SN 2011fe (-1.5 ± 1.5 mJy at $70 \mu\text{m}$). We also analysed archival data described in § 3.1. The measured flux at the SN position in the co-added images is -4.7 ± 6.2 mJy. There is no significant far-IR source evident at the location of the SN before or after the explosion.

3.4 SN 2012cg

SN 2012cg was discovered 2012/05/15.790 by the Lick Observatory Supernova Search at R.A. = 12:27:12.83, Decl. = +09:25:13.2 (J2000) located $17''.3$ East and $1''.5$ South of the peculiar SBa galaxy NGC 4424 at a distance of 15.2 ± 1.9 Mpc (Cortés et al. 2008). SN 2012cg reached a peak B -band magnitude of 12.1 on 2012 June 2. The SN show signs of host galaxy reddening, with a colour excess of $E(B-V) \approx 0.2$ mag derived from both optical photometry and high-resolution spectroscopy (Silverman et al. 2012; Marion et al. 2012).

Our Herschel PACS $70 \mu\text{m}$ and $160 \mu\text{m}$ data from 2012 June 11 (about 9 days after B -band maximum) are shown in Fig. 3. SN 2012cg is located in a region of significant host galaxy far-IR emission. We derive upper limits on possible emission from pre-existing CS dust (Tab. 1) in a similar manner to SN 2011by, by comparing the flux at the SN po-

Table 1. Photometry of SNe 2011by, 2011fe and 2012cg.

Target	Obs. date	PACS band	F_{ν} (mJy)
SN 2011by	2011-05-24	$70 \mu\text{m}$	3.7 ± 1.5
SN 2011by	2011-05-24	$160 \mu\text{m}$	16 ± 8
SN 2011fe	2011-10-03	$70 \mu\text{m}$	-1.5 ± 1.6
SN 2011fe	2011-10-03	$160 \mu\text{m}$	-16 ± 10
SN 2012cg	2012-06-11	$70 \mu\text{m}$	-0.7 ± 1.8
SN 2012cg	2012-06-11	$160 \mu\text{m}$	-23 ± 8

sition with the host galaxy background flux in the absolute vicinity. We measure no excess far-IR emission with respect to the estimated host galaxy background at the location of SN 2012cg (-0.7 ± 1.8 mJy at $70 \mu\text{m}$).

In addition, we also analyse pre-explosion archival PACS $70 \mu\text{m}$ data (described in § 3.1) to look for a possible time dependence of the flux at the location of the SN. After scaling and aligning the pre-SN image to our observations and convolving the post-SN observations with a Gaussian model of the PSF we measure the flux in a $6''$ aperture at the SN location to be -15 ± 5 mJy, which is consistent with the expected background. Due to the large differences in resolution and sensitivity in the pre- and post-explosion images we derive our limits on CS dust from the post-explosion data only.

4 UPPER LIMITS FROM DUST MODELS

To model the far-IR emission from a pre-existing CS dust cloud we consider the idealized case (described in Hildebrand 1983; Fox et al. 2010) of an optically thin dust cloud of mass M_d with dust particles of radius a , emitting thermally at a single equilibrium temperature T_d . The expected flux at a distance D is,

$$F_{\nu} = M_d \frac{\kappa_{\nu}(a) B_{\nu}(T_d)}{D^2}, \quad (1)$$

where $B_{\nu}(T_d)$ is the Planck blackbody function and the dust mass emissivity coefficient, $\kappa_{\nu}(a)$, is

$$\kappa_{\nu}(a) = \left(\frac{3}{4\pi\rho a^3} \right) \pi a^2 Q_{\nu}(a) = \frac{3Q_{\nu}(a)}{4a\rho}. \quad (2)$$

$Q_{\nu}(a)$ is the absorption efficiency and the dust bulk (volume) density, $\rho \approx 2 - 3 \text{ g/cm}^3$ depending on grain composition. The expected emission depends on the choice of dust grain composition and size. Interstellar dust is well described by a mixture of silicate and graphitic grains of different sizes, and generally in the far-IR $\kappa \propto \lambda^{-\beta}$ with $\beta \sim 1 - 2$ and $\kappa \approx 67.0 \text{ cm}^2/\text{g}$ at $70 \mu\text{m}$ (Draine & Li 2001). However, CS dust around SNe may well be dominated by either silicate or graphitic grains depending on the stellar atmosphere of the involved stars. Since we do not know the nature of the SNe Ia progenitor systems and their potential dust production mechanisms, we will consider separate scenarios of either silicate or graphite grains of radius $a = 0.1 \mu\text{m}$ (described in Draine & Lee 1984; Laor & Draine 1993; Weingartner & Draine 2001).

From the non-detections of the SNe in the PACS $70 \mu\text{m}$

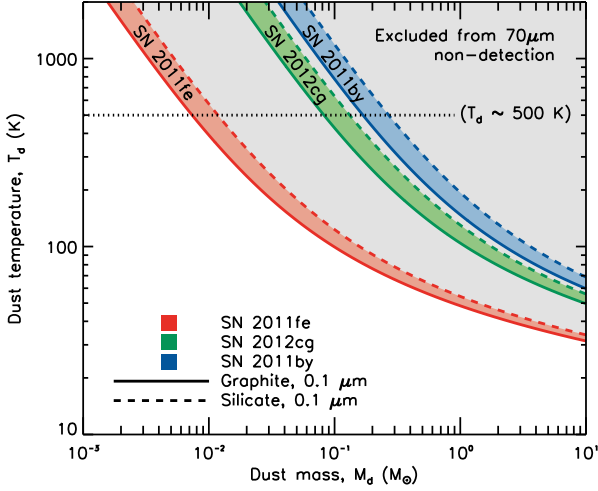


Figure 1. 3σ upper limits on the circumstellar dust mass and temperature, assuming graphitic (solid lines) or silicate (dashed lines) dust grains of size $a = 0.1 \mu\text{m}$, derived from the non-detection in the Herschel PACS $70 \mu\text{m}$ observations of SNe 2011by (blue lines), 2011fe (red lines) and 2012cg (green lines). The horizontal dotted line indicates the expected temperature $T_d \sim 500 \text{ K}$ for a pre-existing dust shell of radius $r_d \sim 10^{17} \text{ cm}$.

and $160 \mu\text{m}$ passbands we calculate upper limits on the CS dust mass surrounding SNe 2011by, 2011fe and 2012cg. The colour corrections to the modeled dust emission spectra for the PACS $70 \mu\text{m}$ and $160 \mu\text{m}$ bands are negligible (maximally $\sim 5\%$).

The upper limits on the dust mass also depend strongly on the dust temperature as illustrated in Fig. 1. To derive an estimate of the expected dust temperatures, we follow the simple IR echo model in Fox et al. (2010). For a typical peak SN bolometric luminosity of $\sim 10^9 L_\odot$, radiatively heating a pre-existing dust shell of radius $r_d \sim 10^{17} \text{ cm}$ (as suggested by e.g. the analysis of Patat et al. 2007), graphitic dust grains of $a = 0.1 \mu\text{m}$ will be heated to $T_d \sim 500 \text{ K}$ (silicate grains would be heated to even higher temperatures).

Due to its proximity, SN 2011fe yields the tightest constraints, $M_d \lesssim 7 \times 10^{-3} M_\odot$ at a 3σ -level, assuming graphitic dust grains of size $a = 0.1 \mu\text{m}$ heated to temperatures $T_d \sim 500 \text{ K}$ (red solid line in Fig. 1). For silicate dust grains, the corresponding upper limit is $M_d \lesssim 10^{-2} M_\odot$ (red dashed line in Fig. 1). The upper limits for SN 2011by are weaker, $M_d \lesssim 10^{-1} M_\odot$ at a 3σ -level for similar assumptions (blue solid and dashed lines for graphitic and silicate dust grains in Fig. 1). For SN 2012cg, the upper limits are $M_d \lesssim 8 \times 10^{-2} M_\odot$ at a 3σ -level for assuming graphitic dust grains of size $a = 0.1 \mu\text{m}$ heated to temperatures $T_d \sim 500 \text{ K}$ (green solid line in Fig. 1).

5 SUMMARY AND CONCLUSIONS

Searches for evidence of CSM around SNe Ia are an important aspect in the efforts to understand the exact nature of these explosions and their use as accurate distance estimators. For the latter, the presence of pre-explosion CS dust could explain the empirically derived, non-standard reddening

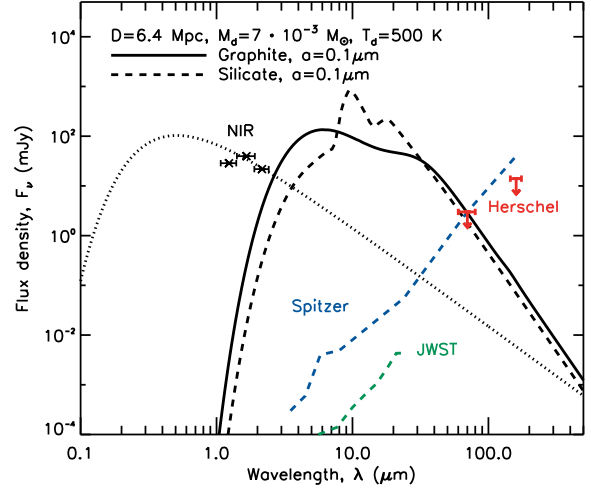


Figure 2. Example of expected IR SEDs of circumstellar dust, assuming a distance of 6.4 Mpc , $M_d = 7 \times 10^{-3} M_\odot$ and $T_d = 500 \text{ K}$ with graphitic (solid black line) or silicate (dashed black line) dust grains of size $a = 0.1 \mu\text{m}$. The dotted black line shows a blackbody spectrum at 10^4 K , scaled to match the NIR fluxes of SN 2011fe 33 days after maximum brightness (Matheson et al. 2012). For comparison, the 5σ detection limits of 3 hr observations with the *Spitzer Space Telescope* (blue dashed line) and the *James Webb Space Telescope* (green dashed line) are included. The red symbols indicate the 3σ upper limits on the flux of SN 2011fe in the PACS $70 \mu\text{m}$ and $160 \mu\text{m}$ bands (described in § 3.3).

ing corrections that are applied to minimize the scatter in the SNe Ia Hubble diagram (Goobar 2008).

In this work, we searched for far-IR emission from pre-existing CS dust around three nearby Type Ia SNe a few weeks after maximum brightness. By considering the Herschel non-detections, we can exclude dust masses $M_d \gtrsim 7 \times 10^{-3} M_\odot$ for dust temperatures $T_d \sim 500 \text{ K}$ at a 3σ -level for SN 2011fe, and the upper limits are one order of magnitude weaker for SNe 2011by and 2012cg, excluding dust masses $M_d \gtrsim 10^{-1} M_\odot$.

The temperature of the heated CS dust depends on the distance to the explosion site. The upper limit on the dust temperature, implied by the evaporation temperature of the dust grains ($T \lesssim 2000 \text{ K}$), corresponds to a minimal dust survival radius $r_{\text{evap}} \sim 10^{16} \text{ cm}$ (Amanullah & Goobar 2011). Detections of CSM around SNe Ia have been reported at somewhat larger distances, $r_{\text{CSM}} \sim 10^{17} \text{ cm}$ (e.g. Patat et al. 2007). CS dust at these radii would be heated to $T_d \sim 500 \text{ K}$. Thermal emission from such CS dust would be essentially negligible in the near-IR, but could potentially be detected at mid-IR wavelengths, e.g. with *Spitzer*. However, the degeneracy with the photospheric emission around $5 \mu\text{m}$ makes it challenging to discern between emission by dust and intrinsic light from the SN, as indicated by Fig. 2. Conversely, observations at $70 \mu\text{m}$ would be completely dominated by radiating dust, which motivates the use of Herschel observations for this study.

Additional aspects that should be considered relate to the timing of the observations. Our observations were carried out within ~ 60 days from explosion, in order to minimize the risk of confusion with dust produced after

the explosion. Nozawa et al. (2011) suggest that significant amounts of dust may condense in the ejecta of SNe Ia around 100 – 300 days after explosion. A second factor is the length of the IR echo, which is expected to scale with the radius of the CS dust shell, $t_{\text{echo}} \sim 2r_d/c$, corresponding to 3 – 4 months for $r_d \sim 10^{17}$ cm. For a geometrically thin, spherically symmetric shell, the fraction of emitting dust mass perceived by the observer increases with time, reaching maximum at $t = t_{\text{echo}}$. Thus, although our observational scheme may miss the IR echo maximum, it nonetheless represents a reasonable compromise for exploring possible pre-existing CS dust shells at $r_d \sim 10^{17}$ cm.

For $r_d \sim 10^{16}$ cm, the IR echo would be too short to be captured by our observations. However, in such a scenario, the CS dust would have been hot enough for its near-IR emission to dramatically change the early part of the observed lightcurves. Thus, Herschel observations for very nearby SNe are complementary to data at shorter wavelengths. While current instrumentation allows mainly for exploration of CS dust around SNe within the very local universe ($D \lesssim 5$ Mpc), forthcoming satellite missions, *JWST* in particular, will have the potential to dramatically improve the sensitivity, as shown in Fig. 2.

The authors are grateful to Hugh Dickinson, Ori Fox, Edvard Mörtsell for useful discussions and comments.

REFERENCES

- Amanullah R., Goobar A., 2011, *ApJ*, 735, 20
 Blondin S., Prieto J. L., Patat F., Challis P., Hicken M., Kirshner R. P., Matheson T., Modjaz M., 2009, *ApJ*, 693, 207
 Chomiuk L. et al., 2012, *ApJ*, 750, 164
 Cortés J. R., Kenney J. D. P., Hardy E., 2008, *ApJ*, 683, 78
 Draine B. T., Lee H. M., 1984, *ApJ*, 285, 89
 Draine B. T., Li A., 2001, *ApJ*, 551, 807
 Folatelli G. et al., 2010, *AJ*, 139, 120
 Foley R. J. et al., 2012, *ApJ*, 752, 101
 Fox O. D., Chevalier R. A., Dwek E., Skrutskie M. F., Sugerman B. E. K., Leisenring J. M., 2010, *ApJ*, 725, 1768
 Gerardy C. L. et al., 2007, *ApJ*, 661, 995
 Gomez H. L. et al., 2012, *MNRAS*, 420, 3557
 Goobar A., 2008, *ApJL*, 686, L103
 Goobar A., Leibundgut B., 2011, *Annual Review of Nuclear and Particle Science*, 61, 251
 Hancock P. P., Gaensler B. M., Murphy T., 2011, *ApJL*, 735, L35
 Hildebrand R. H., 1983, *qjras*, 24, 267
 Horesh A. et al., 2012, *ApJ*, 746, 21
 Immler S. et al., 2006, *ApJL*, 648, L119
 Laor A., Draine B. T., 1993, *ApJ*, 402, 441
 Li W. et al., 2011, *Nature*, 480, 348
 Margutti R. et al., 2012, *ApJ*, 751, 134
 Marion G. H. et al., 2012, *The Astronomer’s Telegram*, 4159, 1
 Matheson T. et al., 2012, *ApJ*, 754, 19
 Nobili S., Goobar A., 2008, *A&A*, 487, 19
 Nozawa T., Maeda K., Kozasa T., Tanaka M., Nomoto K., Umeda H., 2011, *ApJ*, 736, 45
 Nugent P. E. et al., 2011, *Nature*, 480, 344
 Panagia N., Van Dyk S. D., Weiler K. W., Sramek R. A., Stockdale C. J., Murata K. P., 2006, *ApJ*, 646, 369
 Patat F. et al., 2007, *Science*, 317, 924
 Patat F. et al., 2011, *ArXiv e-prints*
 Pilbratt G. L. et al., 2010, *A&A*, 518, L1
 Poglitsch A. et al., 2010, *A&A*, 518, L2
 Russell B. R., Immler S., 2012, *ApJL*, 748, L29
 Shappee B. J., Stanek K. Z., 2011, *ApJ*, 733, 124
 Silverman J. M. et al., 2012, *ApJL*, 756, L7
 Simon J. D. et al., 2009, *ApJ*, 702, 1157
 Sternberg A. et al., 2011, *Science*, 333, 856
 Suzuki N. et al., 2012, *ApJ*, 746, 85
 Tully R. B., Rizzi L., Shaya E. J., Courtois H. M., Makarov D. I., Jacobs B. A., 2009, *AJ*, 138, 323
 Wang L., 2005, *ApJL*, 635, L33
 Weingartner J. C., Draine B. T., 2001, *ApJ*, 548, 296

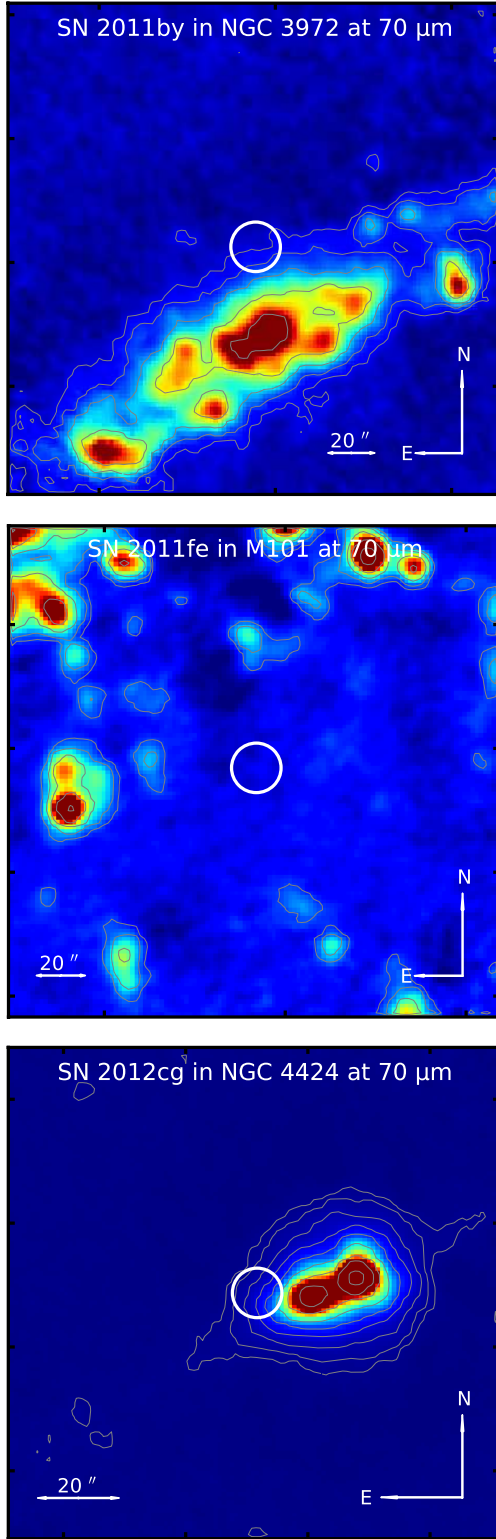


Figure 3. Herschel PACS 70 μm observations of SNe 2011by (top panel), 2011fe (middle panel) and 2012cg (bottom panel). The circles indicate the position of the supernovae and the FWHM of the PSF (6'').